EUROPHYSICS LETTERS 15 October 2005

Europhys. Lett., **72** (2), pp. 242–248 (2005)
DOI: 10.1209/epl/i2005-10237-5

Enhanced He-α emission from "smoked" Ti targets irradiated with 400 nm, 45 fs laser pulses

F. Y. Khattak[1](*), R. J. Clarke[3], E. J. Divall[3], M. Edwards[2], P. S. Foster[3], C. J. Hooker[3], A. J. Langley[3], P. Mistry[2], D. Neely[3], O. A. M. B. Percie du Sert[1], J. Smith[3], C. Spindloe[3], G. Tallents[2], M. Tolley[3] and D. Riley[1]

[1] *School of Mathematics and Physics, Queen's University of Belfast University Road, Belfast, BT7 1NN, UK*
[2] *Department of Physics, University of York - Heslington, York YO10 5DD, UK*
[3] *Central Laser Facility, CLRC Rutherford Appleton Laboratory Chilton, Didcot, Oxon, OX11 0QX, UK*

received 1 July 2005; accepted in final form 31 August 2005
published online 21 September 2005

PACS. 52.38.Ph – X-ray, γ-ray and particle generation.
PACS. 52.25.Os – Emission, absorption, and scattering of electromagnetic radiation.

Abstract. – We present a study of He-like $1s^2$-$1s2p$ line emission from solid and low-density Ti targets under $\simeq 45$ fs laser pulse irradiation with a frequency doubled Ti:Sapphire laser. By varying the beam spot, the intensity on target was varied from 10^{15} W/cm^2 to 10^{19} W/cm^2. At best focus, low density "smoked" Ti targets yield ~ 20 times more He-α than the foil targets when irradiated at an angle of 45° with s-polarized pulses. The duration of He-α emission from smoked targets, measured with a fast streak camera, was similar to that from Ti foils.

Introduction. – Ultra-short laser pulses, created by chirped pulse amplification (CPA) [1], allow for the creation of high density and high temperature plasmas confined to a small volume. The interest in such plasmas is partly driven by their potential for bright short bursts of X-ray radiation [2, 3] with applications in biology and medicine [4, 5], microlithography [6], plasma dynamics [7], X-ray lasers [8], and X-ray diffraction and scattering [9–12]. Efforts to increase the efficiency of such sources, such as modulating the target surface by various means, have been employed, see *e.g.* [13–21]. Rajeev *et al.* [19] have demonstrated 13-fold enhancement in the bremsstrahlung X-ray yield in the (10–200) keV range using targets coated with copper nanoparticles. Nishikawa *et al.* [20] have shown about 10-fold enhancement in the yield of K-α emission from a Si target coated with carbon nanotubes. Their data, however, does not give absolute yields. Kulcsár *et al.* [21] have compared emission from Ni targets with different surface structure and demonstrated a 50 fold increase in the broad-band X-ray yield in the sub-keV region with 1 ps pulses. This was achieved with low density, "smoked" targets which are made by thermal deposition of a metal in an inert atmosphere [22]. They observed that the FWHM of the broad-band XUV (> 150 eV) radiation lasted 70 ps as compared to 25 ps

(*) E-mail: F.Khattak@qub.ac.uk

for nanowire and grating targets and 10 ps from the flat Ni target. For some applications it is desirable to have a quasi-monochromatic source such as K-α or thermal X-ray line emission and we report here an experiment demonstrating enhancement of the line radiation at $\simeq 4.75$ keV with a spectral resolution $\simeq 3$ mÅ and temporal resolution of $\simeq 2$ ps. With single shot time integrated absolute yield data, we demonstrate up to a 20-fold increase in He-α line ($1s^2$ ^1S-$1s2p$ ^1P and satellites) emission (4.7–4.75 keV) from low density "smoked" Ti targets compared to commercially available Ti foils.

Experiment. – The experiments were carried out at the Rutherford Appleton Laboratory using the ASTRA laser facility, delivering up to 0.5 J in 800 nm, p-polarized pulses of $45(\pm 5)$ fs duration. In addition to the pre-pulse activity at $\simeq 13$ ns ahead of the main pulse and having a contrast of 10^{-7}, the main pulse is superimposed on a residual uncompressed pedestal and ASE. The contrast of the residual uncompressed pedestal is measured to be 10^{-6} at 10 ps and rises to 10^{-4} at 1.5 ps ahead of the main pulse. The ASE starts 2 ns ahead of the main pulse, rising linearly from a background of 10^{-8} of the main pulse to a level of 10^{-6}. These measurements were made for the fundamental wavelength of 800 nm (IR) with a third-order autocorrelator. A 0.6 mm thick type-I KDP crystal was employed to convert the IR beam into second harmonic, 400 nm (blue), s-polarized pulses. A beam splitter reflecting the blue and transmitting the IR, was used at 45° to relay the blue beam onto the target. Two dielectric mirrors in the beam-path further reduced the IR component on the target. Such conversion immensely reduces the level of pre-pulse, ASE and CPA pedestal [23] and gives a cleaner laser-solid interaction (the contrast improves as approximately square for the second harmonic). The IR beam hitting the target is reduced by a factor $\simeq 10^6$ and hence IR pedestal level on target is reduced from 10^{-4} to $\sim 10^{-10}$. For the thin crystal used we expect only a few fs increase in pulse width but it was not possible to measure this at 400 nm with an auto-correlator. The conversion efficiency to blue was about 20% and in excess of 60 mJ was achieved on the target. The orientation of the target plane was controlled to select either s- or p-polarized pulses for interaction with the target surface. An f/2.5 off-axis silver-coated parabola was used to focus the 400 nm beam at an angle of 45° from the normal to the target plane. Focal spots at different offsets were recorded in the low energy mode of the laser with an 8-bit CCD coupled with a $\times 40$ microscope objective. The full width at half-maximum (FWHM) of the focal spot at the best focus was measured to be $\simeq 2\,\mu$m containing about 35% of the total energy. A collinear diode laser beam was injected via one of the dielectric mirrors to form the basis of a retro-alignment system that allowed us to find the best focal spot whenever the target foil was moved to a fresh position. The focal spot on target was varied by moving the parabola off the best focus position along the line-of-focus both towards and away from the target (positive off-set and negative off-set, respectively). With negative off-set a convergent beam interacts with the target while in case of the positive off-set the focus lies before the target and a divergent beam interacts with the target. Away from best focus, the focal spot broke up into hot spots and, therefore, the energy distribution in the focal spot changed. The energy on target was monitored via leakage from one of the dielectric mirrors with a fast diode and integrating sphere. At best focus, the intensity reached a maximum of $\simeq 10^{19}$ W/cm^2. We used 12.5 μm thick Ti and smoked Ti deposited on Al substrates as our targets. The smoked targets were fabricated by evaporating Ti in an ambient environment of argon gas at 2–10 Torr. The depth of the Ti deposited on the substrate was $\simeq 20\,\mu$m. The scanning electron micrographs of the foil target and smoked Ti are shown in fig. 1. The surface of the smoked target appeared black in visible light and the micrograph depicts structures having size smaller than the wavelength (400 nm) of the irradiating beam. An AFM scan of the foil target showed a surface smoothness better than 15 nm r.m.s. over the focal area.

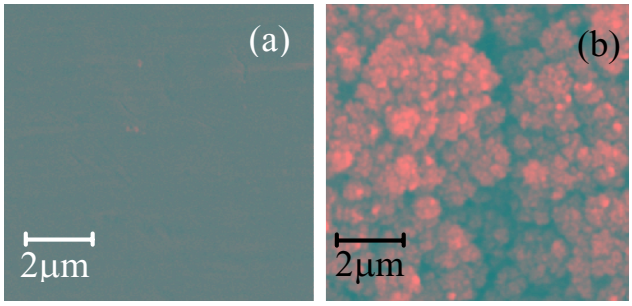

Fig. 1 – SEM micrographs showing the surface of (a) commercially purchased Ti foil target and (b) smoked Ti.

After every shot, the target was moved, by 1 mm for foil and 2 mm for smoked targets, to ensure the beam interacts with a fresh target surface. In all cases, the beam was tight focused on the target, using the retro viewing system, before moving the parabola to the desired offset position. A thin glass pellicle protected the parabola from plasma debris. The time-integrated He-like line emission of Ti was recorded on individual shots with a Von- Hamos crystal (LiF 200) coupled to a 16-bit X-ray CCD system. This system has been calibrated previously at 5.9 keV [24] using an Fe_{55} source. A Von-Hamos PET crystal spectrometer coupled to a Kentech X-ray streak camera with a temporal resolution of 2 ps was used to record the time-resolved He-α emission. The streak camera was fitted with a KBr photocathode and the output was recorded with an intensified CCD system.

Hydrodynamic simulation. – We have simulated plasma conditions, using the one-dimensional hydrodynamic radiation code, HYADES [25], when solid Ti foil is irradiated at an angle of 45° with the uncompressed pedestal and ASE. At the maximum main pulse intensity at-

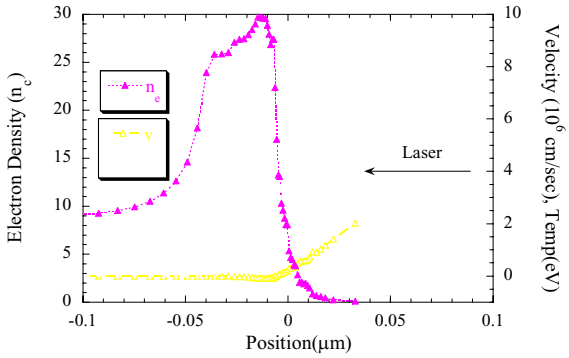

Fig. 2 – Hyades simulated profile of plasma generated by irradiating solid Ti foil with the uncompressed pedestal and ASE when the main pulse intensity level is 3×10^{19} W/cm^2. The wavelength of the laser beam is 400 nm. The zero on the position indicates the initial surface of the solid target.

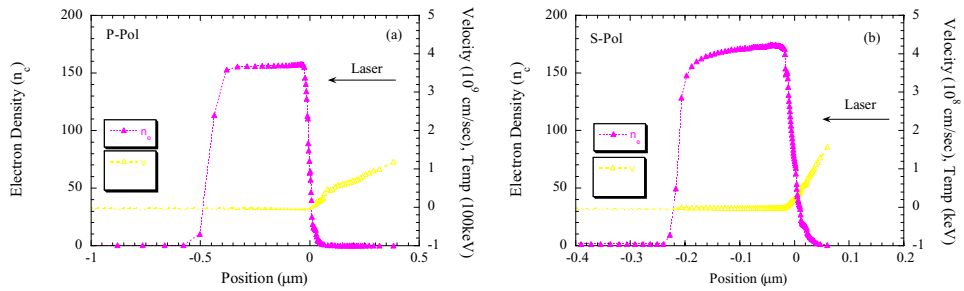

Fig. 3 – Hyades simulated profiles of plasma generated by irradiating the pre-plasma target with 400 nm, 45 fs (a) 45° *p*-polarised, and (b) *s*-polarised pulses. The peak intensity is $3 \times 10^{19}\,\mathrm{W/cm^2}$. The zero on the position indicates the initial surface of the solid target. Note the difference in scales of velocity and temperature for the two cases.

tained in our experiment, *i.e.* ($3 \times 10^{19}\,\mathrm{Wcm^{-2}}$), the uncompressed pedestal will raise to a level of about ($3 \times 10^{11}\,\mathrm{Wcm^{-2}}$) at the arrival of the main pulse. Figure 2 shows the simulated density, temperature, and velocity profile of a plasma generated on the surface of the foil at the arrival of the main pulse. The laser comes from the right and the zero on the position represents the initial solid surface of the Ti foil. As can be seen, the total extension of the plasma is less than $0.1\lambda_0$. The plasma density scale-length at critical surface is $L/\lambda_0 = 0.035$. For such short scale-length plasmas, Brunel's vacuum heating [26] is likely to play a dominant role in coupling laser energy of *p*-polarised pulses to the target. This model estimates absorption of $\simeq 60\%$ at tight focus, falling to $\simeq 10\%$ at 100 μm offset [27]. For the *s*-polarised pulses, we expect collisional absorption at a level of only a few percent for the tight focus [27]. For larger offsets, this level may increase but then the temperature drops which reduces the level of keV emission. Using HYADES, we have also simulated plasma conditions when the 400 nm, 45 fs pulse interacts with the pre-plasma target surface at an angle of 45° and peak intensity of $3 \times 10^{19}\,\mathrm{W/cm^2}$. For this part of our simulation, a Helmholtz wave equation solution package is invoked that uses the frequency-dependent complex dielectric constant for absorption calculation. At the peak of the main pulse, the plasma surface becomes very hot and dense and the scale-length increases to $L/\lambda_0 = 0.12$ for *p*-polarised beam and stays at $L/\lambda_0 = 0.04$ for *s*-polarised beam, as shown in fig. 3(a) and (b), respectively. The energy absorption is about 0.7% for the *s*-polarised and 27% for the *p*-polarised light. As discussed below, this difference in plasma conditions results in higher level of emission for the *p*-polarised case.

Results and discussion. – Figure 4(a) compares absolute He-α yield from a Ti foil and smoked Ti both irradiated with 400 nm, *s*-polarized pulses at 45° incidence as a function of focus position. The data points are an average of 3 or more shots and the standard error bars are shown. The error bar in the focal position is $\pm 20\,\mu$m. The yield at best focus for the smoked targets case corresponds to a conversion efficiency of $\simeq 2 \times 10^{-4}$. At around the best focus, the He-α yield from the smoked Ti target is about 20× greater than that from Ti foil target. In fig. 4(b) we show a similar comparison for *p*-polarized pulses where the results from the two target types are comparable at best focus. However, as can be seen from the error bars, there was a significant shot-to-shot variation in the yield which makes the He emission from foil targets unpredictable. Furthermore, He-α emission from the foil target

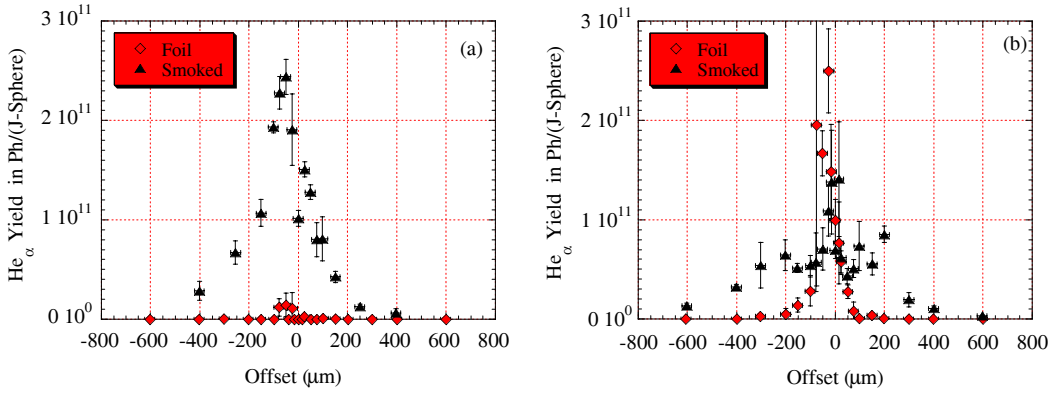

Fig. 4 – Integrated absolute yield of He-α as a function of offset from the best focus for foil and smoked Ti targets irradiated at 45° with (a) s-polarized and (b) p-polarized pulses. The error bars represent standard error in the yield, and fixed error of 20 μm in the offset.

drops very quickly in a FWHM of 50 μm as we go away from the focus, whereas the emission from smoked targets remains high and relatively predictable despite the break-up of the beam, out to more than 200 μm from best focus. From the standard error bars, it seems that the break-up of the beam into hot spots at high defocus does not adversely affect reproducibility significantly. The increased efficiency of p-polarisation over s-polarisation is easily understood for the foil targets. As can be seen from the comparison of figs. 3(a) and (b), the temperature of the surface plasma in case of p-polarised light is about two orders of magnitude higher than in the case of s-polarised pulses. Furthermore, a substantially increased absorption from a few percent for s-polarisation [27] to over 50% for p-polarisation is expected due to the vacuum heating mechanism [26]. In addition super-thermal generated electrons will enhance ionisation and excitation rates in the plasma for p-polarisation.

The optical absorption of smoked targets is expected to be higher than the foil target which is probably the reason for higher efficiency of smoked target, especially at large offsets. The difference in signal between s- and p-polarisation for the smoked targets is at first surprising. The explanation lies in the way in which the electromagnetic field interacts with the non-uniform surface. It is known that high intensity light interacting with nano-scale metal particles can show a resonant enhancement of the field between the particles, see for example refs. [15, 28, 29]. This is a complex interaction but a simplified view for our case might be as follows: For s-polarisation, whatever the angle of incidence, the electric field lies along the surface and thus can drive dipole oscillations in the nano-particle of Ti which can interact with adjacent surface particles to resonantly enhance the field and thus lead to higher levels of non-linear absorption. For the case of p-polarisation at 45 degrees, one component of the electric field is normal to the target surface and thus does not contribute to driving the resonance oscillation of the field and hence results in a lower level of laser target coupling and consequently about half the emission level at the best focus.

In our time-integrated data, the signal is always accompanied by a uniform background covering the entire chip. Since the use of magnets and shielding did not make any difference to the level of the background, and the level varied from shot to shot depending on the focusing

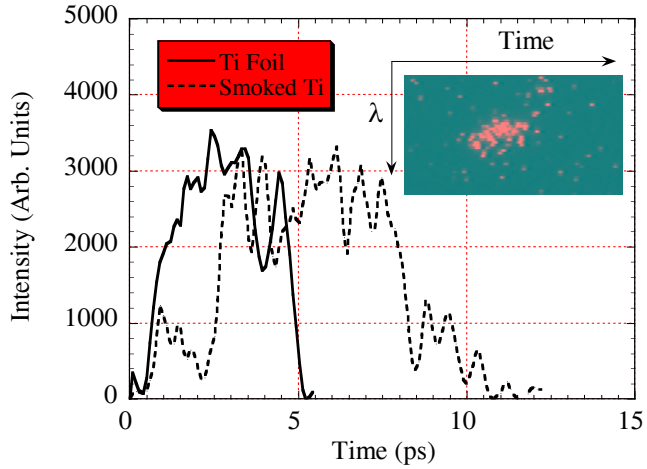

Fig. 5 – Spectrally integrated scans of the time resolved He-α data recorded with a Kentech streak camera coupled to a Von Hamos spectrometer employing a PET crystal. Both the targets were irradiated with 400 nm, 45 fs p-polarized pulses at an irradiance of $\simeq 2 \times 10^{19}$ W/cm^2.The spectral resolution was $\simeq 3$ mÅ and the temporal resolution was $\simeq 2$ ps. The zero on the time scale is arbitrarily chosen. The inset is the raw streak data of He- emission from a foil target.

conditions, we surmise that the background noise on the CCD chip corresponded to hard X-ray fluorescence, probably from the spectrometer and brass substrate. Thus one advantage of irradiating away from best focus with a smoked target is that high He-α yield is obtained with a significant drop in hard X-ray background (by about an order of magnitude at 200 μm defocus).

Figure 5 depicts the spectrally integrated scan of the time-resolved data comparing the emission from the Ti foil and smoked target irradiated with p-polarized pulses at an irradiance of $\simeq 2 \times 10^{19}$ W/cm^2. The spectral resolution was $\simeq 3$ mÅ. The zero on the time scale is arbitrary. Although the satellites and inter-combination line can be seen in the time-integrated spectra they are not readily discernible in the single shot streak data which is noisy due to the low signal level and in any case has a low expected dynamic range (< 10). Thus, fig. 5, in effect, represents the resonance line history. The inset shows raw data of the He-α emission from a foil target, where there is an apparent shift to the blue of $\simeq 4$ mÅ in magnitude during the emission period. This is consistent with a blue shift due to expansion at $\simeq 5 \times 10^7$ cm/s.

The FWHM of the emission is 4 ps and 5.5 ps, respectively for the foil and smoked target. De-convolving these times, using 2 ps as the time resolution of the streak, we get 3.5 ps and 5 ps, respectively. This shows that the duration of He-α emission from the smoked targets irradiated under the conditions discussed is not considerably longer than the emission from the foil targets. This contrasts with broad-band XUV data centred around 25 nm taken with a grating spectrometer (to be published later) which indicated 50–100 ps duration of emission, consistent with observations of Kulcsár *et al.* [21]. The efficiency of our smoked target irradiated with s-polarized pulses to convert optical energy to quasi-monochromatic X-ray emission (4.75 keV) is measured to be $\simeq 2 \times 10^{-4}$ at around the best focus. Pestehe *et al.* [30] have reported an efficiency of $\sim 10^{-5}$ for Ti K-α (4.5 keV) line emission with a duration of ~ 2 ps by irradiating a solid target with 248 nm, 2 ps pulses at an irradiance

of $\simeq 2 \times 10^{16}\,\mathrm{W/cm^2}$. Although the measured duration of emission in our case is somewhat longer than that of Pestehe *et al.* [30], the low signal-to-noise ratio associated with the smoked targets makes this system more suitable for some applications, for example scattering studies.

Conclusion. – In conclusion, we have demonstrated that nano-structured targets can be used to significantly enhance thermal line emission from short pulse plasmas. The advantage over p-polarised irradiation of foils is less clear-cut than for s-polarisation and lies more in the potential for using lower irradiance than in the maximum absolute yield. Furthermore, at 4.75 keV the duration of the line emission was not significantly increased for smoked targets as it is for broad-band sub-keV energies.

* * *

This work was supported by EPSRC grant EP/C001869/01. We would like to thank Dr. A. V. Zayats for helpful discussions.

REFERENCES

[1] Strickland D. and Mourou G., *Opt. Commun.*, **56** (1985) 219.
[2] Kmetec J. D. *et al.*, *Phys. Rev. Lett.*, **68** (1992) 1527.
[3] Reich Ch. *et al.*, *Phys. Rev. Lett.*, **84** (2000) 4846.
[4] Neutze R. *et al.*, *Nature*, **406** (2000) 752.
[5] Svanberg S., *Meas. Sci. Technol.*, **12** (2001) 1777.
[6] Andrew A. A., Ueda T. and Limpouch J., *Proc. SPIE*, **4343** (2001) 789.
[7] Workman J. *et al.*, *Appl. Phys. Lett.*, **70** (1997) 312.
[8] Moon S. J. and Eder D. C., *Phys. Rev. A*, **57** (1998) 1391.
[9] Rischel C. *et al.*, *Nature*, **390** (1997) 490.
[10] Rose-Petruck C. *et al.*, *Nature*, **398** (1999) 310.
[11] Rousse A. *et al.*, *Meas. Sci. Technol.*, **12** (2001) 1841.
[12] Nardi E. *et al.*, *Phys. Rev. E*, **57** (1998) 4693.
[13] Andreev A. A. *et al.*, *Phys. Rev. E*, **65** (2002) 026403.
[14] Nakano H., Nishikawa T. and Uesugi N., *Appl. Phys. Lett.*, **79** (2001) 24.
[15] Murnane M. M. *et al.*, *Appl. Phys. Lett.*, **62** (1993) 1068.
[16] Gordon S. P. *et al.*, *Opt. Lett.*, **19** (1994) 484.
[17] Wülker C. *et al.*, *Appl. Phys. Lett.*, **68** (1996) 1338.
[18] Desai T. *et al.*, *Laser Particle Beams*, **19** (2001) 241.
[19] Rajeev P. P. *et al.*, *Phys. Rev. Lett.*, **90** (2003) 115002-1.
[20] Nishikawa T. *et al.*, *Appl. Phys. B*, **78** (2004) 885.
[21] Kulcsár G. *et al.*, *Phys. Rev. Lett.*, **84** (2000) 5149.
[22] Harris L. and Beasley J. K., *J. Opt. Soc. Am.*, **42** (1952) 134.
[23] Price D. F. *et al.*, *Phys. Rev. Lett.*, **75** (1995) 252.
[24] Khattak F. Y. *et al.*, *J. Phys. D*, **36** (2003) 2372.
[25] Larsen J. T. and Lane S. M., *J. Quant. Spectrosc. Radiat. Transfer*, **51** (1994) 179.
[26] Brunel F., *Phys. Rev. Lett.*, **59** (1987) 52.
[27] Riley D. *et al.*, in *J. Quant. Spectrosc. Radiat. Transfer* (online since 25th May 2005).
[28] Shalaev V. M., *Nonlinear Opics of Random Media*, edited by Höhler G., Vol. **158** (Springer-Verlag, Berlin) 1999.
[29] Gauthier *et al.*, in *Application of Laser Plasma Radiation II*, edited by Richardson Martin C., Kyrala George A., *SPIE Proc.*, Vol. **2523**, 1995, p. 242.
[30] Pestehe S. J. *et al.*, *J. Phys. D*, **35** (2002) 1117.